# Initial Data and Theory for a High Specific-Power Ankle Exoskeleton Device

Sebastian Sovero, Nihar Talele, Collin Smith, Nicholas Cox,
Tim Swift and Katie Byl*

OtherLab Orthotics, San Francisco, CA
{collin,njcox,tim}@otherlab.com
and
Robotics Laboratory, University of California at Santa Barbara (UCSB)
{sesovero,nihar.talele,katiebyl}@gmail.com

**Abstract.** We present experimental data for an ankle exoskeleton that provides a metabolic benefit during running. Intuitively, there is an optimal level of power that any particular human can accept and use to benefit walking or running, which is a function of the particular human, the selected gait, and speed. We provide and discuss modeling optimization results to complement our recent data for the device, toward modifying future designs and understanding theoretical performance limits.

## 1 Introduction

Exoskeletons have been a major thrust of robotics research for nearly two decades, with the goal of assisting an operator during a variety everyday tasks. However, despite this potential, conventional exoskeleton designs such as HULC [1], and XOS2 [2] have proven unable to assist with highly dynamic human behaviors like running, and in many cases walking. As a result, rather than reducing required human effort, these devices turn into expensive, heavy exercise machines, since they increase the metabolic burden associated with movement, which has emerged as a primary metric for performance augmentation applications [3].

Recent work, such as the work under DARPA's Warrior Web program, has made significant strides in this area by advancing a new class of lightweight hardware [4], but even these devices have failed to fully capitalize on the promise of exoskeletons. Despite signicant research efforts, there is only one powered mobile device which was developed at MIT [5] that has demonstrated metabolic assistance in a non-stationary task, and this was for walking. While this is a significant result, arguably the most valuable output from this work is the notion of an "augmentation factor" equation, which predicts the metabolic benefit of an exoskeleton before testing. While this equation may not fully predict the full dynamics of the system, it does provide a vocabulary for comparing the burden of mass and the benefit of added power. In this work, we build off the structure of the augmentation factor equation to evaluate how its major components scale as parameters of human gait speed and device power input vary.

* This work is funded in part through an NSF CAREER Award (CMMI 1255018).

## 2 Technical Approach

The augmentation factor equation introduced in [5], shown below, estimates the metabolic benefit an exoskeleton provides to a human during locomotion, due to the combined effects of Augmentation Power (AP) from both added power and dissipative effects and of Power to Carry (PC) due to the location-dependent effects of the added mass of a device that the human user must carry.

$$AF = \underbrace{\frac{p^+ - p_{dist}}{\eta^+}}_{AP} - \underbrace{\sum_i \beta_i m_i}_{PC} \tag{1}$$

At the center of our work here is a realization that the two principal components (mass and power) of the augmentation factor equation are only understood in a very limited context. Specifically, the existing data that are used to capture the metabolic burden of added mass are only accurate for walking at 1.25 m/s, although it seems more intuitive to assume the effect should be velocity-dependent (i.e., $\beta_i = \beta_i(v)$). Similarly, the metabolic benefit provided by the added power is represented as linear across all powers and at all forward speeds. Toward better understanding mass and power effects of a lower-limb exoskeleton, we structured a set of modeling optimizations along with two human subject studies to capture the fundamental aspects of these principal components, for use across a wider variety of operating cases.

### 2.1 Simulations

Recent works using local optimization methods (e.g., Sequential Quadratic Programming or Interior Point methods) have produced a variety of compelling results in the field of legged robotics, particularly toward developing and/or investigating energy efficient gaits [6–8]. These methods have also been demonstrated to translate well to real physical systems, subject to a variety of constraints and objective functions, as demonstrated by multiple teams within the recent DARPA Robotics Challenge (DRC) [9–11]. Here, we use optimization of a seven-link planar biped model to investigate the effects of added mass across a range of walking speeds and for different locations of added mass on each leg.

### 2.2 Added Mass Study

For the burden of added mass, we had a pilot study of 10 unimpaired subjects (8 male, 2 female, 26.1 ± 3.1 years, weight 77.2 ± 11.9 kg, height 1.78 ± .07 meters) to evaluate the metabolic burden of added mass throughout walking (1.25 m/s and 1.75 m/s) and running speeds (2.25 m/s and 2.75 m/s). We tested a variety of masses ranging from .45 kg to 3.18 kg on various locations. The masses were placed bilaterally above and below each leg joint (ankle, knee, hip) to simulate the weight of a exoskeleton actuator. The motivation was to build a data set for an exoskeleton designer so that actuator placement and design can be optimized.

### 2.3 Added Power Study

For the benefit of added power, we studied three subjects with varying power levels at running and walking speeds. The exoskeleton (Fig. 1) delivers high peak powers at the ankle. Our preliminary data corresponds to an ankle joint muscle-tendon "apparent efficiency" [12] of $\eta^{+}_{ankle} = .30$ (mechanical watt per metabolic watt) at 2.8 m/s running for the lower power range,where $\eta^{+}_{ankle} = \frac{Average\ exoskeleton\ positive\ mechanical\ power}{\Delta\ Net\ human\ metabolic\ power}$.

**Fig. 1.** The Otherlab exoskeleton utilizes cloth pneumatic actuators for toe off. This novel cloth actuator functions equivalently to an pneumatic expansion cylinder, but with much lower added weight.

With regard to assistive power, Mooney et al. suggest power has a linear effect on the metabolic burden; however, a simple thought experiment leads to the hypothesis that there is a point where you begin to see diminishing returns from adding power to the operator. For a given design, extremely low levels of assistance power result in a metabolic burden because not enough power is put in to overcome the mass of the device. Similarly, if too much power is introduced to the leg, exoskeleton "assistance" likely disrupts an operator's natural biomechanics. This may create a metabolic burden at high levels of power. In between, there is an ideal amount of added mechanical power that the operator can accept and leverage without disrupting their biomechanics. This hypothesized shape is depicted by the green dashed line in Fig. 11. We suspect that such diminishing returns have not yet been observed because all published beneficial exoskeletons have output less than 30W at the ankle [12].

## 3 Results

### 3.1 Simulations

For the simulations, the seven-link planar walker shown in Fig. 2 was constructed using mass, inertia and length parameters taken from [13, p. 302] so that the model resembles a 74.2 kg human. The walker has 2 actuators at the hips, 2 at knees and 2 at ankles. We used a partial feedback linearization (PFL) based controller and designed trajectories using $4^{th}$-order polynomials to generate a walking motion. Parameters for the polynomials were then optimized to minimize the cost of transport. We used the fmincon solver with the interior point algorithm in Matlab for these

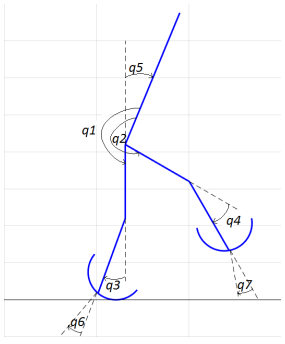


**Fig. 2.** 7-link walker model

optimizations. Cost of Transport (CoT) was calculated by adding the absolute values of both positive and negative work at the joints and always dividing by the mass of the unburdened biped model. Figures 3 and 4 show the effects of adding increasing amounts of mass at each limb at either the lower shank of the leg (i.e, at the ankle) or the lower portion of the thigh (just above the knee), with walking speed constrained at 1.3 (m/s), while Figures 5 and 6 show how CoT varies as a function of speed. Here, the simulation is constrained to a walking (i.e., non-running) gait.

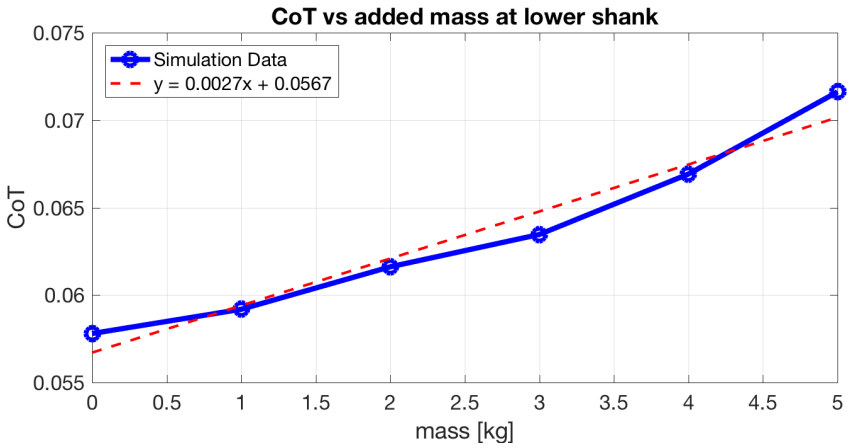


**Fig. 3.** Cost of transport(CoT) versus total mass added bilaterally to the lower shank. These simulation data were taken for walking at 1.3 m/s.

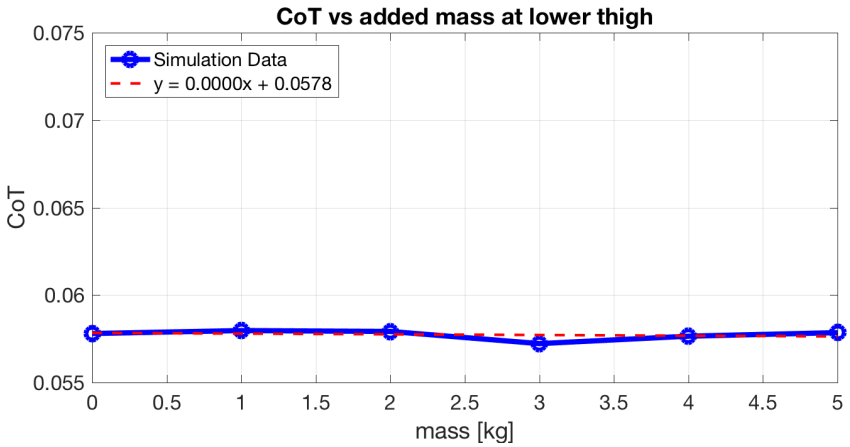


**Fig. 4.** Cost of transport(CoT) versus total mass added bilaterally to the lower thigh. These simulation data were taken for walking at 1.3 m/s.

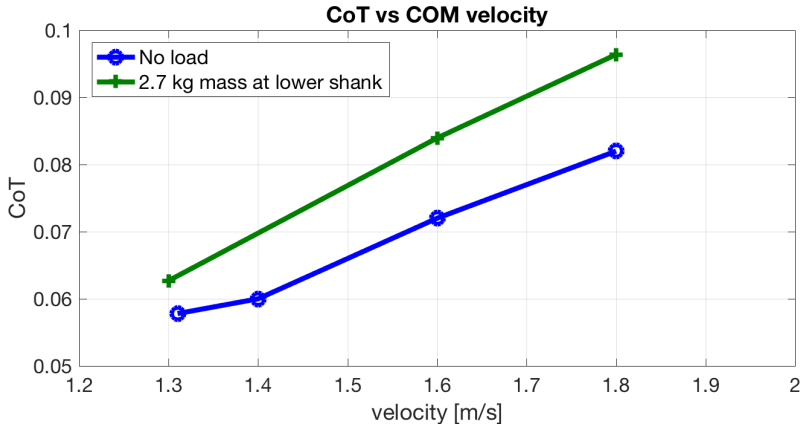


**Fig. 5.** Variation of Cost of Transport (CoT) due to change in walking speed with and without load. A total load of 2.7 kg was added bilaterally to lower shank for each simulation optimization data point.

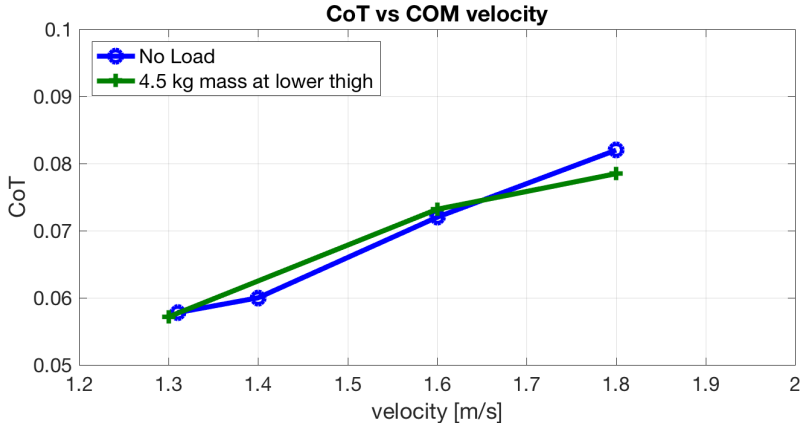


**Fig. 6.** Variation of Cost of transport(CoT) due to change in walking speed with and without load. A total load of 4.5 kg was added bilaterally to lower thigh for each simulation optimization data point.

### 3.2 Added Mass Study

Figures 7 and 8 show human subject data when the total mass shown on the x-axis is distributed bilaterally at either the lower shank (just above the ankle) or lower thigh, respectively. Figures 9 and 10 show how human energy consumption varies as a function of locomotion speed, both with and without added mass.

Note that for both these experimental data and the corresponding simulation optimizations (Figures 3 through 6), adding mass at the more distal location is both more costly and more velocity-dependent (slope of data), and that the

effects of varying velocity are approximately linear across walking speeds, as theoretically anticipated. At the higher two velocities tested in both Figures 9 and 10, subjects were performing a running gait. Simulating analogous results for running remains a task for future work.

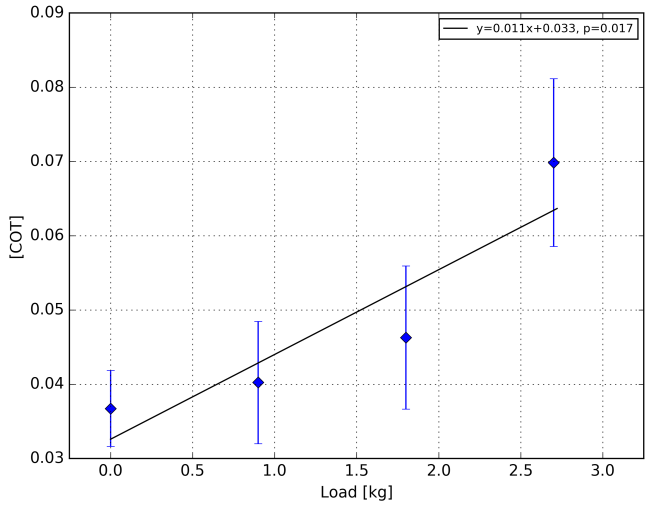


**Fig. 7.** Experimental data for mass added to the lower shank. The energy is normalized for the subject walking at 1 m/s. This data is for subjects walking at 1.25 m/s.

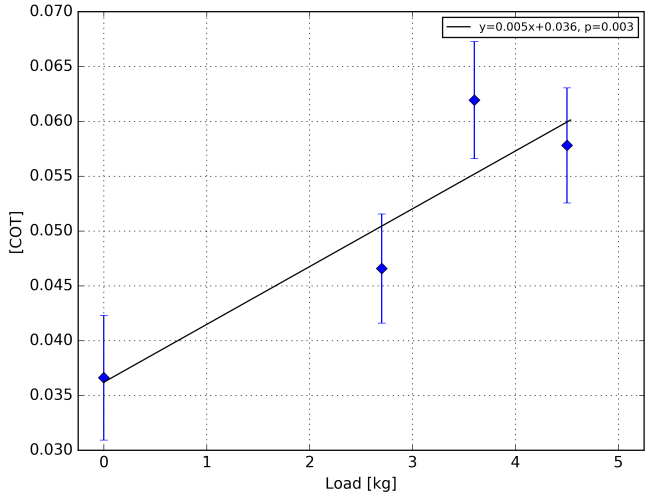


**Fig. 8.** Experimental data for mass added to the lower thigh. The energy is normalized for the subject walking at 1 m/s. This data is for subjects walking at 1.25 m/s.

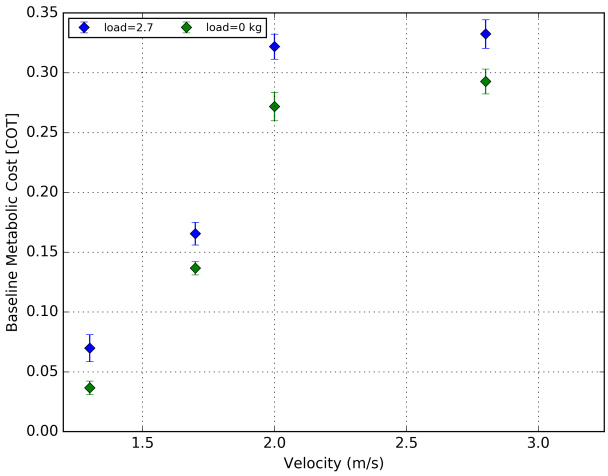


**Fig. 9.** Cost of transport for strapping a total mass of 2.7 kg bilaterally to the lower shank. Notice that the burden seems to grow with forward speed. The subjects were asked to walk at 1.25 and 1.75 m/s, and only run at 2.0 and 2.75 m/s.

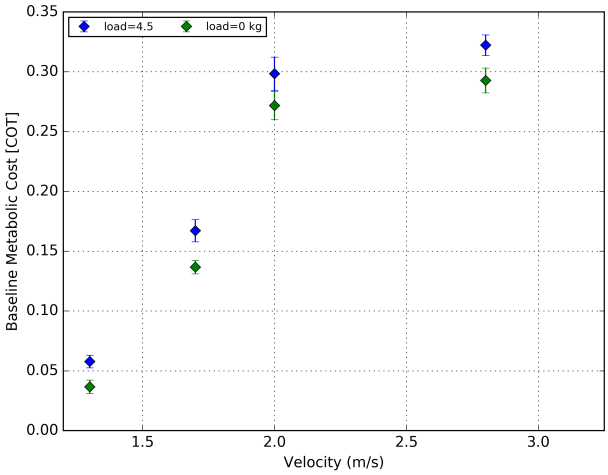


**Fig. 10.** Cost of transport for strapping a total mass 4.5 kg bilaterally to the lower thigh. Notice that the burden seems to grow with forward speed. The subjects were asked to walk at 1.25 and 1.75 m/s, and only run at 2.0 and 2.75 m/s.

While the biped simulations lack much of the details of a true human – for example neglecting upper limb motion, simulating foot contact with a rolling arc, and constraining motion to the sagittal plane – they arguable capture and support general trends within the human subject data. For example, adding mass at the lower thigh (vs the ankle) requires surprisingly little additional energy

during locomotion. In fact, if one divides by the total system mass (including the human plus added mass) in simulation, COT actually goes down as mass is added, indicating humans would walk more efficiently with a different mass distribution, increasing mass near the knees. Also, human effort increases with a significant slope as walking speed approaches the preferred walk-to-run transition speed (Figs. 9 and 10) but is comparatively flat for different running speeds, as previously noted in the literature [14, Fig. 9.3]. Finally, if one assumes a muscle efficiency of around 25% [15], we would expect a human would require on the order of four (i.e., 1/0.25) times the energy predicted in our simulations. This is in general agreement with a slope of 0.011 in Fig. 7 vs 0.0027 in Fig. 3.

### 3.3 Added Power Study

Our aim throughout is to understand the effects of two aspects of exoskeleton design: added power and added mass. A key insight is that high specific power, i.e., a high power to weight ratio, is more essential than simply providing more power alone, due in particular to the burden of added mass near the ankle. In this section, we present initial data to examine the effects of added power.

Below are results from human testing performed at Otherlab. Data in Figure 11 documents the first demonstration of metabolic benefit from an exoskeleton during running gaits. Although these data comprise a limited set of trials, the results are very promising.

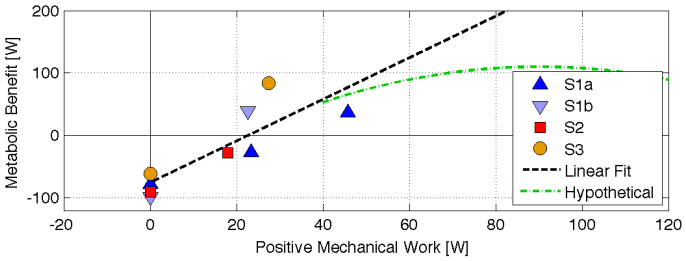


**Fig. 11.** Individual responses to positive mechanical power supplied by (and with the added mass burden of) the exoskeleton. On average, subjects used 1100 W to run unassisted at 2.8 m/s. Data were taken from subjects running at 2.8 m/s. There were 9 tests distributed across 3 subjects (S1,S2,S3). A least squares interpolation yields $y = 3.34x - 75.9$ with $R^2$=0.84, suggesting this may be the first exoskeleton to produce a metabolic benefit while running. The green dashed line qualitatively depicts diminishing returns we suspect will occur at unknown higher power levels.

## 4 Conclusions

Our recent experimental data indicate that we have made the first metabolically beneficial powered running exoskeleton. Coupled with additional simulation data and added mass human studies, we have provided initial clues to explain why our device succeeds where so many others have failed. In particular, both simulations

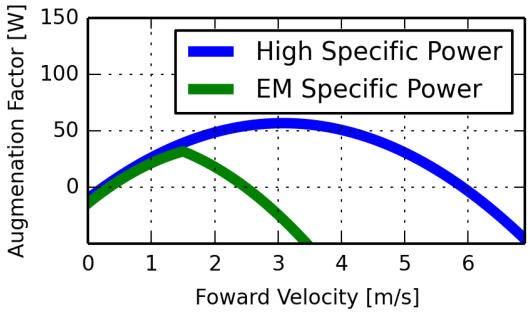


**Fig. 12.** This cartoon figure illustrates a comparison of two devices of the same mass, but different power capacities. A higher specific power can deliver more power for the same mass, resulting in usefulness over a larger range of speeds. In contrast, a electromechanical (EM) device can only offset it's mass burden at slow walking speeds. The corner in the green curve comes from the power saturation. At this point, mass burden grows, but power supplied by the device remains static.

and human subject data show the increased impact of adding mass distally, near the ankle and foot. In contrast, the data also show a surprisingly low burden associated with a location just above the knee. These findings deserve further study and may significantly influence design of future exoskeletons, particularly when power must be carried on board.

Our studies have been designed to expand and refine the augmentation factor equation. Future revisions to the equation building upon this work should enable designers to quantitatively balance the power and mass of an exoskeleton more effectively. This understanding will allow exoskeleton designers to optimize performance more effectively, minimizing the arduous prototype and test cycle. The central dilemma to an exoskeleton mechanical design is weighing the added power and the burden of added weight. This dilemma is captured succinctly with one attribute: the specic power of the actuation architecture being used. To demonstrate this, consider an example design similar to that in Mooney et al. [5] that is a single ankle design sized to provide around 25 W of positive mechanical power to maximize benefit for a 1.5 m/s walk.

This single design necessarily has a fixed mass across all velocities. This design creates two limits: at velocities less than the design velocity (1.5 m/s) the augmentation factor is limited by how much power the operator can accept, while at higher velocities the augmentation factor is limited by the peak power of the actuator. These two limits result in a peak achievable augmentation factor and a defined range of velocities where the device can provide metabolic neutrality or better. In contrast, a high specific power alternative with a comparable mass but significantly increased peak power capacity can greatly increase the available augmentation capability. As a result, the recent push towards lightweight exoskeletons has been somewhat misguided. Achieving high augmentation factors

across a wide range of velocities cannot be done solely by focusing on reducing weight of a design; a more essential aspect is to provide actuation with higher specic powers – more power with less weight.

## References


1. Lockheed Martin, "HULC." [Online]. Available: http://www.lockheedmartin.com/us/products/exoskeleton/hulc.html
2. Raytheon, "XOS2." [Online]. Available: \url{http://www.army-technology.com/projects/raytheon-xos-2-exoskeleton-us/}
3. K. Amundson, "Human exoskeleton control and energetics," Ph.D. dissertation, UC Berkeley, Berkeley, CA, USA, 2007.
4. M. Wehner, B. Quinlivan, P. M. Aubin, E. Martinez-Villalpando, M. Baumann, L. Stirling, K. Holt, R. Wood, and C. Walsh, "A lightweight soft exosuit for gait assistance," in *Robotics and Automation (ICRA), 2013 IEEE International Conference on*. IEEE, 2013, pp. 3362–3369.
5. L. M. Mooney, E. J. Rouse, and H. M. Herr, "Autonomous exoskeleton reduces metabolic cost of human walking during load carriage," *Journal of neuroengineering and rehabilitation*, vol. 11, no. 1, p. 1, 2014.
6. L. Righetti, J. Buchli, M. Mistry, M. Kalakrishnan, and S. Schaal, "Optimal distribution of contact forces with inverse-dynamics control," *International Journal of Robotics Research*, vol. 32, no. 3, pp. 280–298, 2013.
7. I. Mordatch, J. M. Wang, E. Todorov, and V. Koltun, "Animating human lower limbs using contact-invariant optimization," *ACM Transactions on Graphics (TOG)*, vol. 32, no. 6, p. 203, 2013.
8. M. Posa, C. Cantu, and R. Tedrake, "A direct method for trajectory optimization of rigid bodies through contact," *International Journal of Robotics Research*, vol. 33, no. 1, pp. 69–81, 2014.
9. S. Karumanchi, K. Edelberg, I. Baldwin, J. Nash, B. Satzinger, J. Reid, C. Bergh, C. Lau, J. Leichty, K. Carpenter, M. Shekels, M. Gildner, D. Newill-Smith, J. Carlton, J. Koehler, T. Dobreva, M. Frost, P. Hebert, J. Borders, J. Ma, B. Douillard, K. Shankar, K. Byl, J. W. Burdick, P. Backes, and B. Kennedy, "Team robosimian: Semi-autonomous mobile manipulation at the 2015 darpa robotics challenge finals," *J Field Robotics: Special Issue on the 2015 DRC Finals*, 2016.
10. C. Liu, C. G. Atkeson, S. Feng, and X. Xinjilefu, "Full-body motion planning and control for the car egress task of the darpa robotics challenge," in *IEEE-RAS 15th Int. Conf. on Humanoid Robots (Humanoids)*. IEEE, 2015, pp. 527–532.
11. S. Kuindersma, R. Deits, M. Fallon, A. Valenzuela, H. Dai, F. Permenter, T. Koolen, P. Marion, and R. Tedrake, "Optimization-based locomotion planning, estimation, and control design for the atlas humanoid robot," *Autonomous Robots*, vol. 40, no. 3, pp. 429–455, 2016.
12. G. S. Sawicki and D. P. Ferris, "Mechanics and energetics of incline walking with robotic ankle exoskeletons," *J of Exp Biology*, vol. 212, no. 1, pp. 32–41, 2009.
13. A. Tözeren, *Human body dynamics: classical mechanics and human movement*. Springer Science & Business Media, 1999.
14. A. A. Biewener, *Animal locomotion*. Oxford University Press, 2003.
15. D. J. Farris and G. S. Sawicki, "The mechanics and energetics of human walking and running: a joint level perspective," *J of The Royal Society Interface*, 2011, doi: 10.1098/rsif.2011.0182.